Materials Science and Engineering A 528 (2011) 2239–2245

Contents lists available at ScienceDirect

Materials Science and Engineering A

journal homepage: www.elsevier.com/locate/msea

High strain rate characteristics of 3-3 metal–ceramic interpenetrating composites

Hong Chang[a,*], Jon Binner[a], Rebecca Higginson[a], Paul Myers[b], Peter Webb[c], Gus King[c]

[a] Department of Materials, Loughborough University, UK
[b] Dyson Thermal Technologies, Sheffield, UK
[c] Permali (Gloucester) Ltd., Gloucester, UK

ARTICLE INFO

Article history:
Received 6 May 2010
Received in revised form 5 October 2010
Accepted 5 December 2010
Available online 10 December 2010

Keywords:
Interpenetrating composites
Split Hopkinson's pressure bar
Depth of penetration
Damage characterisation

ABSTRACT

3-3 interpenetrating composites (IPCs) are novel materials with potentially superior multifunctional properties compared with traditional metal matrix composites. The aim of the present work was to evaluate the high strain rate performance of the metal–ceramic IPCs produced using a pressureless infiltration technique through dynamic property testing, viz. the split Hopkinson's pressure bar (SHPB) technique and depth of penetration (DoP) analysis, and subsequent damage assessment. Though the IPCs contained rigid ceramic struts, the samples plastically deformed with only localised fracture in the ceramic phase following SHPB. Metal was observed to bridge the cracks formed during high strain rate testing, this latter behaviour must have contributed to the structural integrity and performance of the IPCs. Whilst the IPCs were not suitable for resisting high velocity, armour piercing rounds on their own, when bonded to a 3 mm thick, dense Al_2O_3 front face, they caused significant deflection and the depth of penetration was reduced.

1. Introduction

For an armour tile to be effective, it needs both high penetration resistance and the capability of withstanding more than a single impact. Whilst a high compressive strength is a fundamental requirement for a light armour, the lack of ductility in tension is sometimes the cause for the catastrophic failure [1]. Typically, although ceramics are attractive materials for ballistic applications in terms of their abrasion resistance, which can blunt/erode the incoming projectiles and absorb the energy, hence defeating the threat, they have poor multi-hit potential, shattering after as little as one impact and needing to be replaced [2]. Such deficiencies can be at least partially addressed nowadays via the use of a mosaic approach and constraint.

On the other hand, metal matrix composites (MMCs) have been shown to display a number of useful properties for a wide range of different applications, including improved strength, stiffness, hardness, light weight, wear and abrasion resistance, lower thermal expansion coefficients and better resistance to elevated temperatures and creep compared to the matrix metal, whilst retaining adequate electrical and thermal conductivity, ductility, impact and oxidation resistance [3–5]. As a result, they are being increasingly used in applications such as aerospace and defence components [6–9].

Amongst the MMCs, 3-3 interpenetrating composites (IPCs) consisting of 3-dimensionally interpenetrating matrices of metallic and ceramic phases are interesting materials with potentially superior properties compared with traditional dispersed phase composites [10]. One of the most widely used methods to fabricate IPCs is the infiltration of molten metals into ceramic foams or powder beds [11]. Whilst infiltration under pressure, such as squeeze casting, offers high efficiency, it has difficulty in fabricating complex shaped components and risks damaging the ceramic preform. Pressureless infiltration approaches avoid these limitations [12]. By careful control of the thermo-atmospheric cycle and the use of precursor coatings, a range of molten aluminium alloys can be successfully infiltrated into a number of ceramic foam compositions, including alumina, mullite and spinel [13–15]. Properties of the IPCs have been studied by the authors, which have shown promising wear resistance, as well as flexural properties and ductility [16,17]. However, the high strain rate performance of the IPCs is yet to be studied.

The objective of the present work was to manufacture IPCs using the pressureless infiltration technique and then to evaluate their performance using both SHPB and DoP approaches. The effect of the density of the precursor Al_2O_3 foams on the subsequent high strain

* Corresponding author at: College of Engineering, Mathematics and Physical Sciences, University of Exeter, North Park Road, Exeter, UK.
E-mail address: H.chang@exeter.ac.uk (H. Chang).

0921-5093/$ – see front matter © 2010 Elsevier B.V. All rights reserved.
doi:10.1016/j.msea.2010.12.016

rate performance of the composites was studied and the resulting damage to the system was thoroughly assessed.

2. Experimental

2.1. Processing

The precursor Al_2O_3 foams were supplied by Dyson Thermal Technologies, Sheffield, UK. Made by gel casting an aqueous suspension of two grades of Al_2O_3 powders with mean particle sizes of 0.5 μm (CT3000, SG, Alcoa Industrial Chemicals Europe, Frankfurt, Germany), and 6 μm (MDS-6, Panadyne™, Pennsylvania, USA) in a ratio of 10 to 1, the foams measured 70 mm in diameter by 10 mm thick and had densities of 15–35% of theoretical and cell sizes in the range of 50–200 μm. An Al–8 wt.% Mg alloy, selected on the basis of previous research [15], was used as the infiltrant. Whilst full details of the process route are described elsewhere [15,18], in brief the Al_2O_3 foam samples were placed on top of similarly shaped and sized discs of the alloy, the metal–ceramic couples being contained in alumina boats. These were heated at 20 °C min^{-1} in flowing Ar in a tube furnace; the ceramic foam was infiltrated with the metal in a tube furnace at 915 °C in pure N_2. A holding time of 30–60 min was sufficient for complete infiltration. One additional series of samples was made in which individual 10 mm diameter 3 mm thick, slip cast, dense alumina discs were attached to Al–Mg/15% Al_2O_3 IPCs *in situ* during the infiltration process by providing excess metal which formed an interfacial layer between the ceramic front face and IPC backing. Microstructural observation revealed that the process worked extremely well with the foam being completely infiltrated and the ceramic facing being bonded onto the IPC with no gaps or residual porosity.

2.2. High strain rate evaluation

Initial evaluation of the high strain rate characteristics of the composites was carried out using the split Hopkinson's pressure bar (SHPB) technique, on samples measuring 9 mm in diameter and 4.5 mm in thickness. The stress–strain curve of the composite was obtained from the analysis of the incident wave, the reflective wave and the transmitted wave [19]. Three sets of strain rates were aimed to be produced by using three different apertures in the sealing plug, namely, apertures of Φ8 mm, Φ12 mm and Φ20 mm. Due to the different characteristics of the samples selected, i.e. ceramic content hence hardness, the strain rates calculated following the SHPB test varied amongst groups of samples. The Al–Mg/30% Al_2O_3 IPC, in particular, showed lower strain rates than the others whilst further attempts to achieve higher strain rates in this IPC often resulted in damage in the strain sensors embedded on the bars. The depth of penetration, DoP, ballistic evaluation of the composites was performed by Permali (Gloucester) Ltd. using 7.62 mm, steel tipped, armour piercing (AP) rounds at a velocity of 700 ± 20 ms^{-1}. The composites were glued onto an aluminium backing with a thickness of ~50 mm. The residual energy of the bullet after passing through the target composite was indicated quantitatively by the depth of penetration of the round into the backing, this was ascertained by cutting the backing aluminium in half to reveal the DoP.

2.3. Microstructure characterisation and damage assessment

For polarized light microscopy, the IPCs were ground and polished metallographically using diamond paste and then anodized using 5% fluroboric acid at 20 V for about 90 s. For Scanning Electron Microscopy (SEM) observation (1530VP FEG SEM, LEO Elektronenskopie GmbH, Oberkochen, Germany), the samples were given a final polish using 0.02 μm colloidal silica prior to observation. TEM foils (examined using a 2000FX, Jeol, Tokyo, Japan) were specifically prepared from the metal–ceramic interface using a Dual Beam Focused Ion Beam (FEI – Nanolab 600, FEI Europe, Eindhoven, The Netherlands) from both SHPB and DoP tested composites; the latter samples were produced from near the impact site.

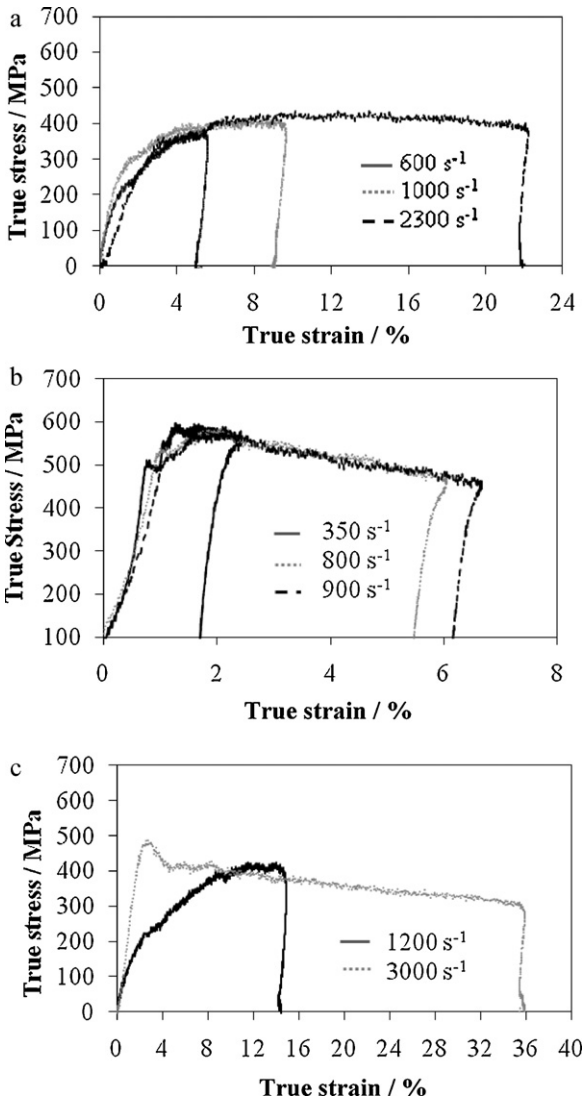

Fig. 1. True stress–strain curves of (a) Al–Mg/15% Al_2O_3, 50–100 μm average cell diameter; (b) Al–Mg/30% Al_2O_3, 50–100 μm average cell diameter; and (c) Al–Mg/25% Al_2O_3, 100–200 μm average cell diameter.

3. Results

3.1. Ballistic testing

Representative SHPB results are shown in Fig. 1. Although the IPCs contained a continuous Al_2O_3 network throughout their structure, they yielded at ~1–2% strain then displayed plastic deformation, behaviour more typical of a metallic material, and they remained macroscopically intact without shattering or falling apart. With an increase of strain rate, the yield strength of all the IPCs increased, showing strain rate sensitivity of the yield strength. For the Al–Mg/15% Al_2O_3 IPC, the curves are all of very similar shapes and the increase in the strain is purely a result of a higher impact velocity. With an increase in ceramic content in the IPC, the yield strength and the maximum true stress observed increased monotonically, obeying the role of mixture. The Al–Mg/30% Al_2O_3

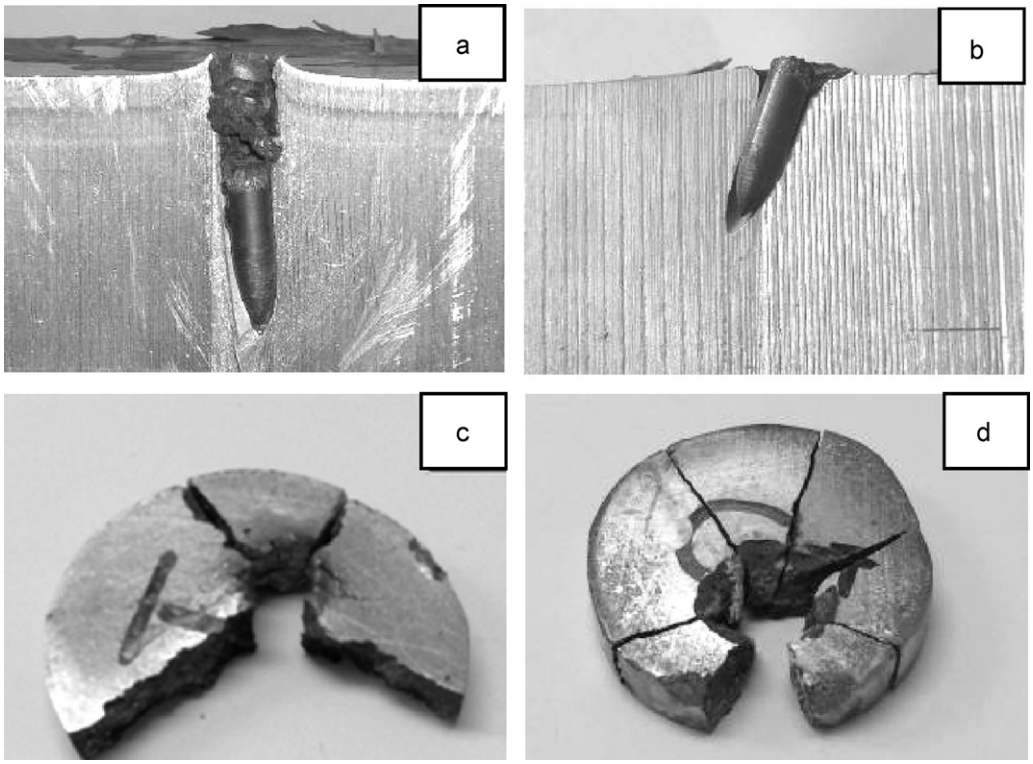

Fig. 2. Samples after ballistic testing, (a) Al backing after ballistic test with no IPC present; (b) Al backing after ballistic test with an Al–Mg/25% Al_2O_3 IPC; (c) Al–Mg/15% Al_2O_3 IPC; and (d) Al–Mg/30% Al_2O_3 IPC. All samples had an average cell diameter of 50–100 μm.

IPC had the highest values of ~500 MPa and 600 MPa for yield strength and true stress, respectively, but the degree of strain decreased. The true stress in the sample also showed a fairly rapid decrease with increasing strain following the initial increase on initiation of the test; a similar trend is observed in the Al–Mg/25% Al_2O_3 IPC (Fig. 1(c)) at the higher strain rate. This suggests that the interpenetrating ceramic structure might have suffered the initiation of microcracking/fracture; a result supported by the fact that the spherical pores in the sintered ceramic structure were deformed by the SHB test (see Fig. 4).

The Al–Mg/25% Al_2O_3 IPC, Fig. 1(c), exhibited strain rate sensitivity, and with an intermediate ceramic content, the samples are 'perfect' transition from the Al–Mg/15% Al_2O_3 IPC to the Al–Mg/30% Al_2O_3 IPC when subjected to different strain rates: at the lower strain rate, the deformation seemed more metallic deformation dominated as the Al–Mg/15% Al_2O_3 IPC, whilst at the higher strain rate, the role and/or microcracking of the ceramic seemed more predominant. It should be noted that the samples have a slightly larger cell size of 100–200 μm in average, compared to 50–100 μm in average in Fig. 1(b) and (c). It would be interesting to investigate the response of the IPCs with various cell sizes in future.

The depths of penetration of the IPCs after ballistic tests are shown in Table 1; selected images of the samples after testing may be seen in Fig. 2. Whilst the IPCs on their own are insufficient to stop a high velocity round and the DoP values change little, the results with respect to deflection for the IPCs produced from 25 and 30% dense Al_2O_3 foam were considered very encouraging, Fig. 2(a and b). Once the round hit the composite, the hard, continuous Al_2O_3 network deflected the round and hence contributed to the resistance to penetration. Spall deformation of the composites produced from 15% dense foam was observed at the periphery of the impact site, Fig. 2(c), a phenomenon often observed in metallic targets [20]. The IPCs made from 30% dense foam, Fig. 2(d), though generally fractured into more fragments, were more effective in deflecting

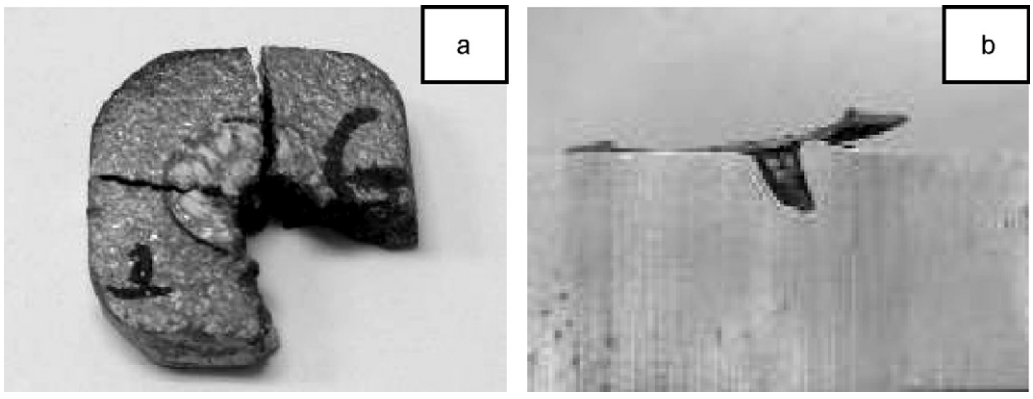

Fig. 3. Al–Mg/15% Al_2O_3 IPC produced with a 3 mm dense Al_2O_3 disc bonded to the surface, (a) the sample after ballistic testing; (b) the Al backing after testing. Note in (b) that the sample has detached from the backing.

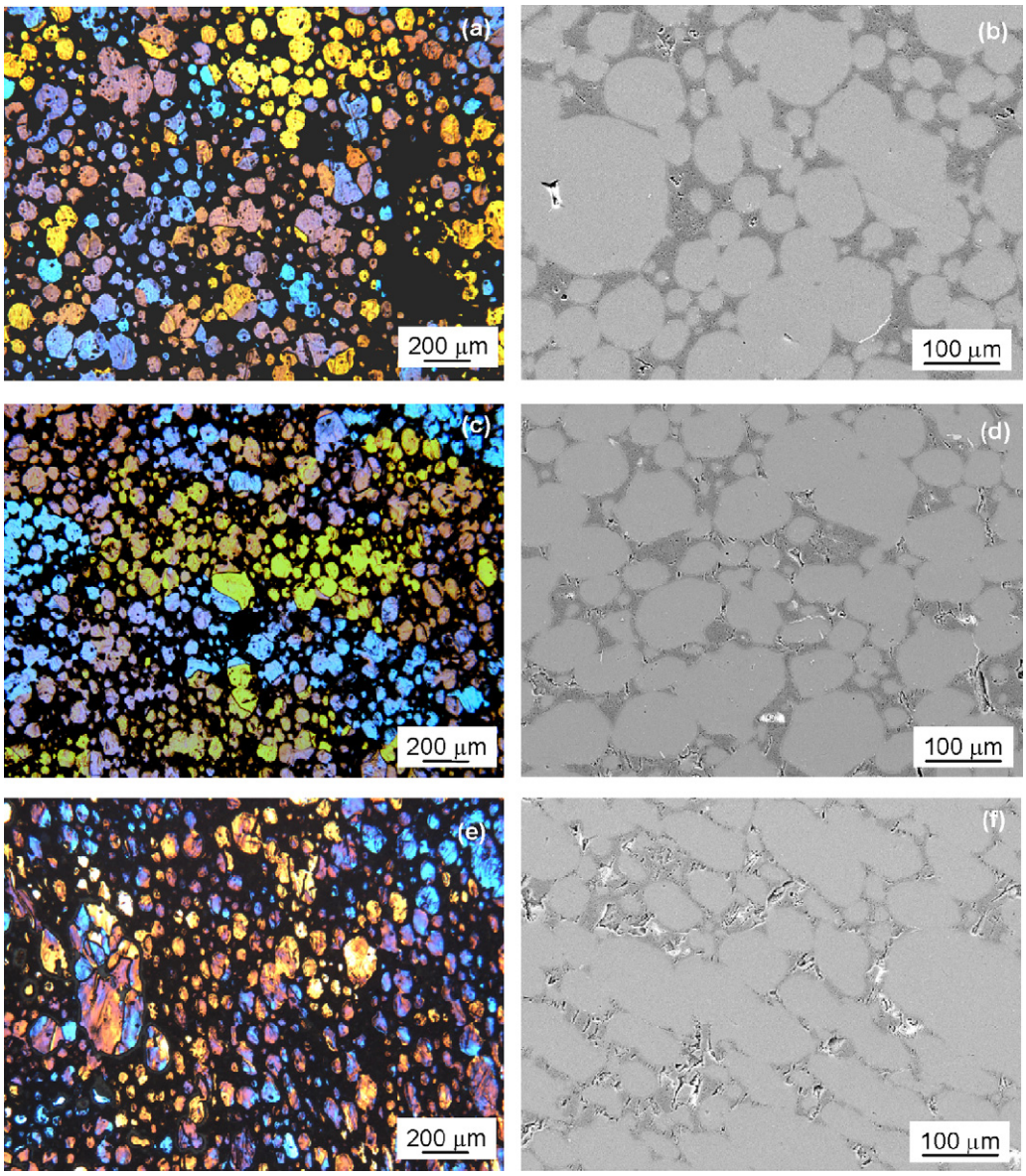

Fig. 4. Optical and SEM micrographs of the Al–Mg/15% Al_2O_3 IPC after SHPB testing at (a and b) 600 s^{-1}; (c and d) 1000 s^{-1} and (e and f) 2300 s^{-1}.

the round and hence reducing the penetration depth. This is correlated with the SHPB results in Fig. 1(b) that the sample had a higher compressive yield strength.

The results, however, were surpassed by the ballistic performance of the Al–Mg/15% Al_2O_3 IPC produced with a Ø10 × 3 mm, slip cast, dense Al_2O_3 disc *in situ* bonded to the surface by using excess metal during the infiltration stage. It deflected the round by 30° and had a DoP value of just 12.4 mm, Table 1, though the IPC sheared off the aluminium backing, Fig. 3. Clearly, the combination of a hard ceramic facing and a ductile IPCs transition effectively

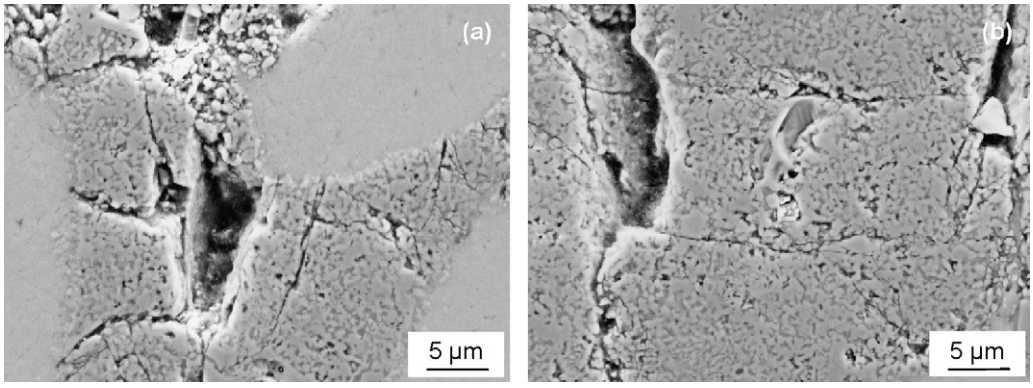

Fig. 5. SEM micrographs of an Al–8Mg/25% Al_2O_3 IPC after SHPB testing.

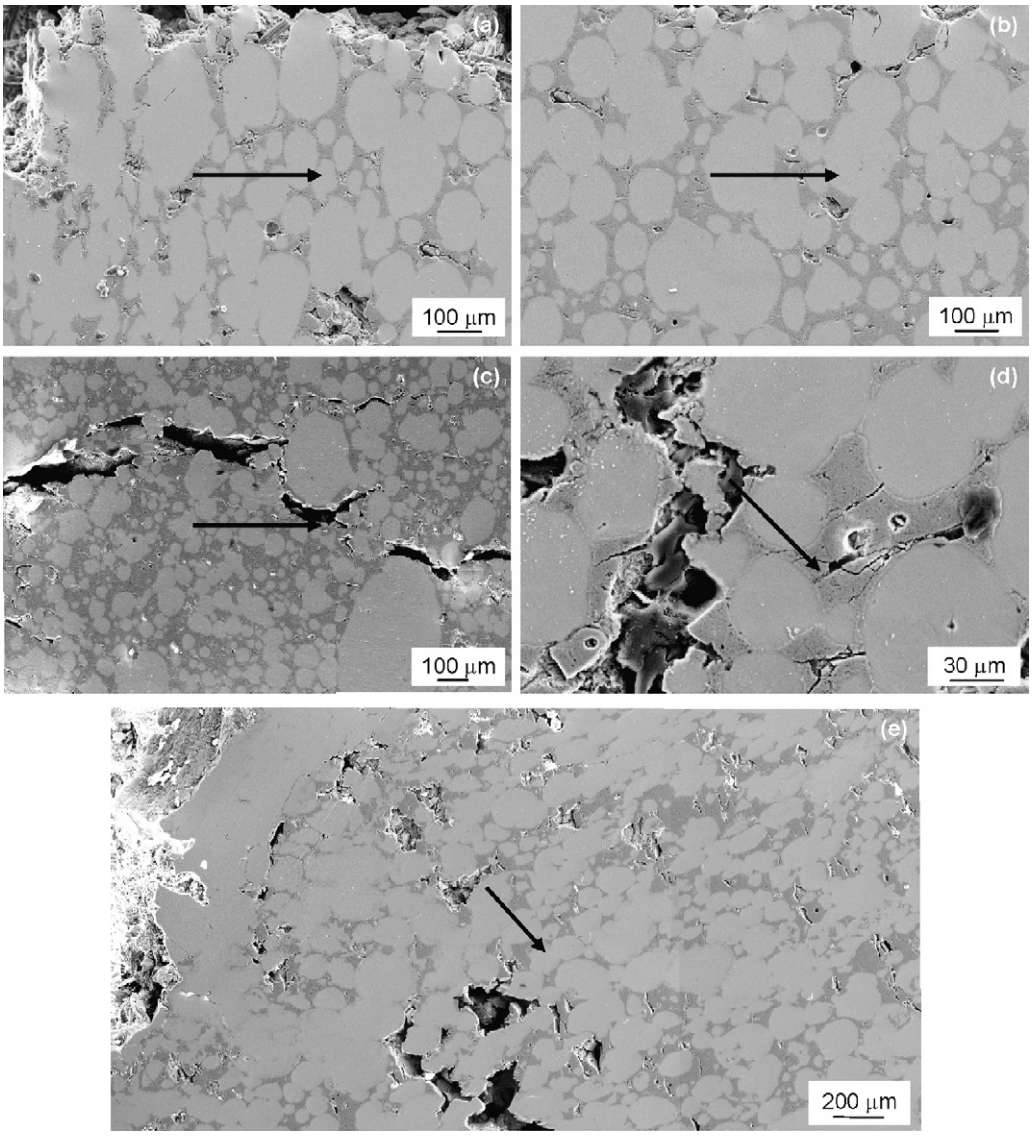

Fig. 6. SEM micrographs of the IPCs after DoP testing: (a and b) Al–Mg/15% Al_2O_3; (c and d) Al–Mg/30% Al_2O_3; and (e) Al–Mg/15% Al_2O_3 with 3 mm dense Al_2O_3 front layer. The arrows indicate the general direction of the stress wave.

improved the ballistic performance. What's more, when there is a ceramic front face, acoustic impedance mismatches at the resulting interfaces can be a cause of significant problems since the stress waves from the ballistic event are reflected back inside the ceramic as tensile waves, causing its rapid destruction [21]. The ballistic properties of ceramic-faced armours have been widely studied [22–25], the presence of a functionally gradient layer between the ceramic front face and metal back face can make the acoustic impedance change less abrupt resulting in less damage from reflected tensile forces [21,26]. It is possible that the attachment of the IPC to the dense Al_2O_3 layer may have reduced the acoustic impedance mismatch of an otherwise more abrupt transition from Al_2O_3 to Al alloy backing, resulting in the superior ballistic performance of the samples.

3.2. Microstructure characterisation

Optical images and SEM micrographs of Al–Mg/15% Al_2O_3 IPCs tested under various strain rates in the SHPB test are shown in Fig. 4. The surfaces observed are parallel to the compression direction, hence the deformation of the original spherical cells into ellipses may be clearly observed. The samples plastically deformed with only localised fracture in the ceramic phase. The cracks appear parallel to the compression direction as a result of tensile stresses. No

Table 1
Results of DoP ballistic tests.

IPC composition	Avg cell size/μm	Avg DoP[a]/mm	Deflection
Al alloy backing	–	36.6 ± 0.2	0°
Al–Mg/15% Al_2O_3	50–100	24.7 ± 0.2	0–7°
Al–Mg/30% Al_2O_3	50–100	23.5 ± 0.2	5–17°
Al–Mg/15% Al_2O_3 with 3 mm dense Al_2O_3 face	50–100	12.4 ± 0.2	30°

[a] Depth into aluminium backing alloy.

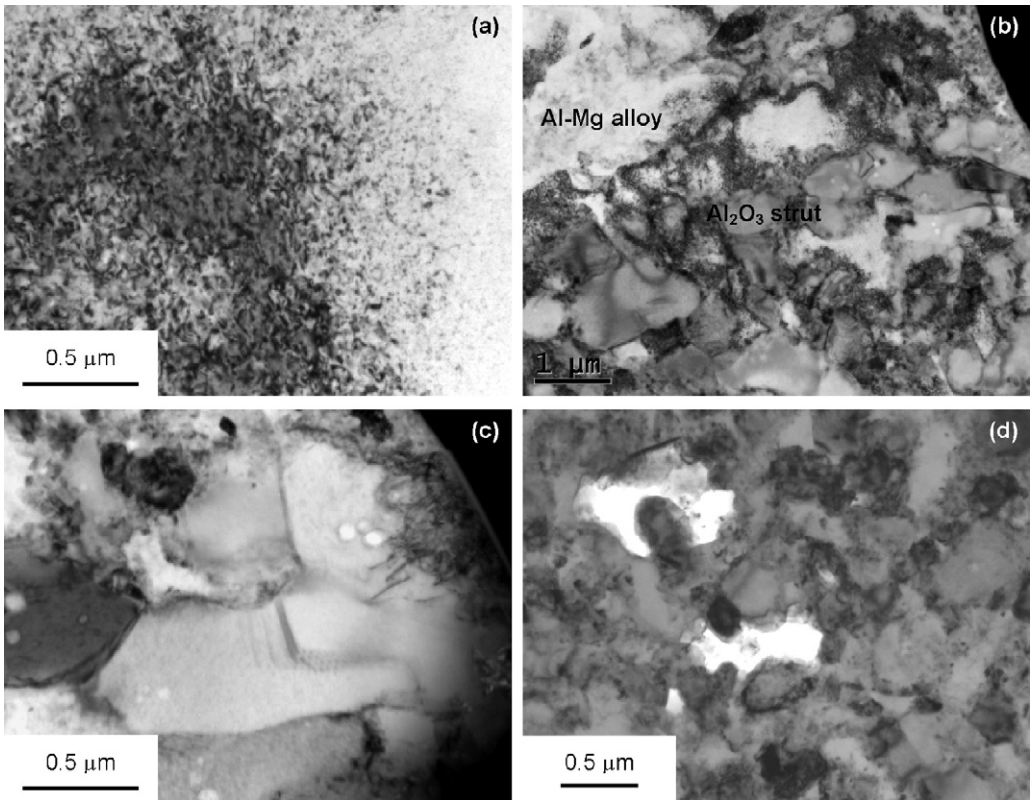

Fig. 7. TEM micrographs of the IPCs after high strain rate testing: (a) the Al–Mg alloy, (b) the metal–ceramic interface, (c) the ceramic struts, all after DoP testing, and (d) the ceramic struts after SHPB testing.

macroscopic metal–ceramic interfacial debonding was observed, rather the cracks stop at the metal–ceramic interface with the latter remaining intact. Similar toughening effect from the metal phase was observed in the IPCs tested using 3-point bending method [17]; electron backscatter diffraction (EBSD) analysis revealed that as with Fig. 4, the alloy had a large grain size with single grains generally inhabiting multiple cells, which can introduce plastic deformation occurring within a group of neighbouring cells hence absorbing more energy than that could have been achieved if each cell had contained an independent metal grain. In Fig. 4(e) and (f), at the highest strain rate of 2300 s^{-1}, the compression of the Al alloy is evident; the foam struts fractured locally and penetrated into the softer Al, preventing the fragmentation of the whole sample.

Fig. 5 shows the SEM micrographs of the Al–Mg/25% Al_2O_3 IPCs at higher magnifications. Thin secondary cracks between the two main cracks are observed in Fig. 5(a). The Al_2O_3 grains fractured mainly intergranularly, whilst transgranular fracture of the Al_2O_3 may occur in bigger grains, Fig. 5(b).

Micrographs of the IPCs after DoP testing are shown in Fig. 6; the arrows indicate the general direction of the stress wave. In Fig. 6(a), an IPC made from 15% dense Al_2O_3 reveals that the original spherical cells were deformed to ellipsoids near the point of impact in a similar manner to the SHPB test. The degree of deformation decreased along the impact wave transmission direction towards the edges of the sample, Fig. 6(b). In contrast, the composites produced from 30% dense Al_2O_3 showed barely any deformation of the spherical cells, Fig. 6(c); the crack originates from the point of impact. The metal may be observed to bridge the crack in the image, Fig. 6(c) and (d), which must have contributed to the structural integrity and performance of the IPCs. For the IPC made from 15% dense foam and protected by a 3 mm thick dense Al_2O_3 front layer, the composite beneath the front face was protected from major radial cracks, Fig. 6(e), whilst the deformation of the original spherical cells into ellipsoids did occur as with Fig. 6(a) indicating energy absorption by the IPCs. Despite the IPCs containing a continuous, brittle Al_2O_3 network, the samples exhibited significant plastic deformation with only minor cracks in the foam struts after testing and the alloy–ceramic interfaces remained intact with no interfacial debonding being observed.

Typical TEM micrographs at the metal–ceramic interface of the SHPB and DoP samples are shown in Fig. 7. From Fig. 7(a), tremendous numbers of dislocations were formed in the metal alloy with both SHPB and DoP testing, as expected. In the Al_2O_3 struts as is shown in Fig. 7(b), a large number of dislocations were formed in the metallic phase along the Al_2O_3 grain boundaries (detailed TEM microstructure of the IPCs can be found in [18]) whilst few dislocations were formed in the Al_2O_3 grain in DoP tested samples, Fig. 7(c), and no dislocations were observed in the Al_2O_3 struts in SHPB-tested samples, Fig. 7(d). This difference in the presence of dislocations in the Al_2O_3 struts is probably due to the lower degree of plastic deformation originating during the SHPB test, however, it should also be noted that due to batch to batch variations, the ceramic foams used for the two tests had different grain sizes (that in the SHPB samples was finer, Fig. 7(d)); this may also have contributed to the difference in dislocation density after the tests.

4. Conclusions

Al–Mg/Al_2O_3 interpenetrating composites have been produced by the pressureless infiltration of Al_2O_3 foams with densities in the range of 15–35% of theoretical and average cell diameters of the order of 50–200 μm. The ballistic properties of the IPCs have been assessed using both SHPB and DoP techniques and the resulting damage in the samples evaluated by a range of microscopy techniques. The results have shown that, on their own, the IPCs are not suitable for resisting high velocity, armour piercing rounds,

however, when bonded to a 3 mm thick, dense Al_2O_3 front face, they caused significant deflection and the depth of penetration was reduced, promising for a graded armour.

Though the IPCs contained rigid ceramic struts, the samples plastically deformed with only localised fracture in the ceramic phase. The cracks were parallel to the compression direction, which indicates that they were formed as a result of tensile stresses. No macroscopic metal–ceramic interfacial debonding was observed, rather the cracks stopped at the metal–ceramic interface with the latter remaining intact. When made from 15% dense Al_2O_3 foams, the original spherical cells were deformed to ellipsoids near the point of impact, the degree of deformation decreasing along the impact wave transmission direction towards the edges of the sample. In contrast, the IPCs produced from 30% dense Al_2O_3 foams showed barely any deformation of the spherical cells. Metal was observed to bridge the cracks formed during high strain rate testing, this latter behaviour must have contributed to the structural integrity and performance of the IPCs.

Acknowledgements

The authors gratefully acknowledge funding from the EPSRC in the UK; Dyson Thermal Technologies, Sheffield, UK, for supplying the alumina foams and Permali (Gloucester) Limited, Gloucester, UK for the ballistic testing and valuable advice.

References

[1] M.L. Wilkins, C.F. Cline, C.A. Honodel, Report No. UCRL-50694, Lawrence Livermore National Laboratory, Livermore, CA, 1969.
[2] K.S. Kumar, M.S. DiPietro, Scr. Metall. Mater. 32 (1995) 793–798.
[3] S.C. Tjong, Z.Y. Ma, Mater. Sci. Eng. R 29 (2000) 49–113.
[4] R.B. Bhagat, M.F. Amateau, M.B. House, K.C. Meinert, P. Nisson, J. Compos. Mater. 26 (1992) 1578–1593.
[5] M. Manoharan, J.J. Lewandowski, Acta Metall. Mater. 38 (1990) 489–496.
[6] S.P. Rawal, JOM 53 (2001) 14–17.
[7] W.S. Lee, W.C. Sue, J. Compos. Mater. 34 (2000) 1821–1841.
[8] S. Abkowitz, D.M. Rowell, H.L. Heussi, H.P. Ludwig, S.A. Kraus, US Pat. No. 4987033, 1991.
[9] J.M. McCauley, G. D'Andrea, K. Cho, M.S. Burkins, R.J. Dowding, W.A. Gooch, ARL-SR-143, 2006.
[10] D.R. Clarke, J. Am. Ceram. Soc. 75 (1992) 739–759.
[11] A. Mortensen, in: T.W. Clyne (Ed.), Metal Matrix Composites, Elsevier, 2000, pp. 521–554.
[12] M.K. Aghajanian, M.A. Rocazella, J.T. Burke, S.D. Keck, J. Mater. Sci. 26 (1991) 447–454.
[13] R. Soundararajan, G. Kuhn, R. Atisivan, S. Bose, A. Bandyopadhyay, J. Am. Ceram. Soc. 84 (2001) 509–513.
[14] J.W. Liu, Z.X. Zheng, J.M. Wang, Y.C. Wu, W.M. Tang, J. Lü, J. Alloy Compd. 465 (2008) 239–243.
[15] J.G.P. Binner, H. Chang, R.L. Higginson, J. Eur. Ceram. Soc. 29 (2009) 837–842.
[16] H. Chang, J.G.P. Binner, R.L. Higginson, Wear 268 (2010) 166–171.
[17] H. Chang, R.L. Higginson, J.G.P. Binner, J. Mater. Sci. 45 (2010) 662–668.
[18] H. Chang, R.L. Higginson, J.G.P. Binner, J. Microsc. 233 (2009) 132–139.
[19] H. Kolsky, Proc. Phys. Soc. Lond. Ser. B 62 (1949) 676–700.
[20] T. Børvik, S. Dey, A.H. Clausen, Inter. J. Imp. Eng. 36 (2009) 948–964.
[21] A. Tasdemirci, I.W. Hall, Inter. J. Imp. Eng. 34 (2007) 1797–1813.
[22] D. Sherman, T. Ben-Shushan, Int. J. Imp. Eng. 21 (1998) 245–265.
[23] J. López-Puente, A. Arias, R. Zaera, C. Navarro, Inter. J. Imp. Eng. 32 (2005) 321–336.
[24] E. Straßburger, B. Lexow, O. Beffort, R. Jeanquartier, in: 19th International Symposium of Ballistics, Interlaken, Switzerland, 2001.
[25] M. Lee, Y.H. Yoo, Inter. J. Imp. Eng. 25 (2001) 819–829.
[26] E. Medvedovski, Adv. Appl. Ceram. 105 (2006) 241–245.